ACS chemical biology

Articles

pubs.acs.org/acschemicalbiology

Hsp90 C-Terminal Inhibitors Exhibit Antimigratory Activity by Disrupting the Hsp90α/Aha1 Complex in PC3-MM2 Cells

Suman Ghosh,[†] Heather E. Shinogle,[‡] Gaurav Garg,[†] George A. Vielhauer,[§] Jeffrey M. Holzbeierlein,[§] Rick T. Dobrowsky,[∥] and Brian S. J. Blagg*[,†]

[†]Department of Medicinal Chemistry, [‡]Microscopy and Analytical Imaging Laboratory, [∥]Department of Pharmacology and Toxicology, The University of Kansas, Lawrence, Kansas 66045, United States

[§]Department of Urology, The University of Kansas Medical Center, Kansas City, Kansas 66160, United States

Supporting Information

ABSTRACT: Human Hsp90 isoforms are molecular chaperones that are often up-regulated in malignances and represent a primary target for Hsp90 inhibitors undergoing clinical evaluation. Hsp90α is a stress-inducible isoform of Hsp90 that plays a significant role in apoptosis and metastasis. Though Hsp90α is secreted into the extracellular space under metastatic conditions, its role in cancer biology is poorly understood. We report that Hsp90α associates with the Aha1 co-chaperone and found this complex to localize in secretory vesicles and at the leading edge of migrating cells. Knockdown of Hsp90α resulted in a defect in cell migration. The functional role of Hsp90α/Aha1 was studied by treating the cells with various novobiocin-based Hsp90 C-terminal inhibitors. These inhibitors disrupted the Hsp90α/Aha1 complex, caused a cytoplasmic redistribution of Hsp90α and Aha1, and decreased cell migration. Structure−function studies determined that disruption of Hsp90α/Aha1 association and inhibition of cell migration correlated with the presence of a benzamide side chain, since an acetamide substituted analog was less effective. Our results show that disruption of Hsp90α/Aha1 interactions with novobiocin-based Hsp90 C-terminal inhibitors may limit the metastatic potential of tumors.

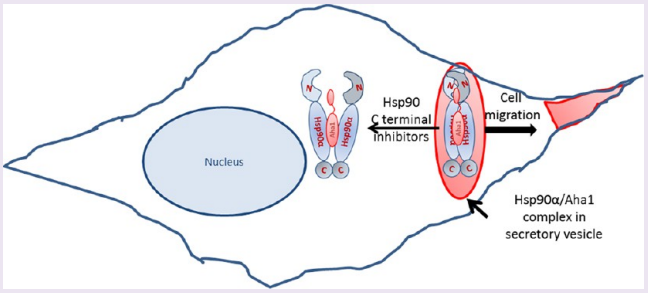

Cell migration is a central process in the development and maintenance of multicellular organisms and controls biological processes such as embryonic development, wound healing, immune responses, tumor formation, and metastasis. Cell migration can be broadly divided into polarization, protrusion, adhesion, regulation and integration, and cell body translocation and retraction of the rear. Establishment and maintenance of cell polarity is a critical first step in cell migration and metastasis. At the leading edge of a migrating cell, rapid actin polymerization is required for lamellipodia formation. From the lamellipodia in migrating cells, slender cytoplasmic projections called filopodia are extended.[1−3] Filopodia play roles in sensing, migration, cell−cell interactions, and adhesion.[4] The proteins involved in cell migration undergo spatiotemporally regulated turnover[5] and need to be folded rapidly to function properly.

Hsp90 (heat shock protein 90) is an evolutionarily conserved molecular chaperone that is responsible for the conformational maturation of nascent polypeptides and the stabilization of mature proteins. In mammals, the Hsp90 family has been broadly divided into four isoforms that serve distinct cellular functions: Hsp90α (HSP90AA1), Hsp90β (HSP90AB1), glucose-regulated protein 94 (Grp94 or HSP90B1), and tumor necrosis factor receptor-associated protein 1 (TRAP1). Hsp90α is stress inducible and responsible for the maturation of proteins that are expressed or denatured during cellular insult. Hsp90α has been reported to undergo secretion and promote metastasis of tumors.[6−10] Recent evidence suggests that during apoptosis, Hsp90α becomes phosphorylated and colocalizes with DNA-dependent protein kinase at the apoptotic ring, near the edge of the nucleus.[11] Because of its role in cancer, Hsp90α represents an excellent target for the development of anticancer agents. Hsp90β is highly homologous to Hsp90α but is constitutively expressed and responsible for the maturation and degradation of proteins required for normal cellular maintenance.[12] Grp94 is found in the endoplasmic reticulum, and in addition to its role in protein processing, it is essential for the maturation of secretory and membrane proteins.[13,14] TRAP1 is localized to the mitochondria and functions to protect against oxidative stress.[15,16]

Hsp90, the chaperone Hsp70, and several other proteins termed co-chaperones form dynamic complexes known as the Hsp90 chaperone machinery. Cancer cells use the Hsp90 chaperone machinery to protect mutated or overexpressed oncoproteins, which aids in the progression of cancer.[17] Hsp90 co-chaperones bind both the N- and C-termini of the protein

Received: August 14, 2014
Accepted: November 17, 2014
Published: November 17, 2014

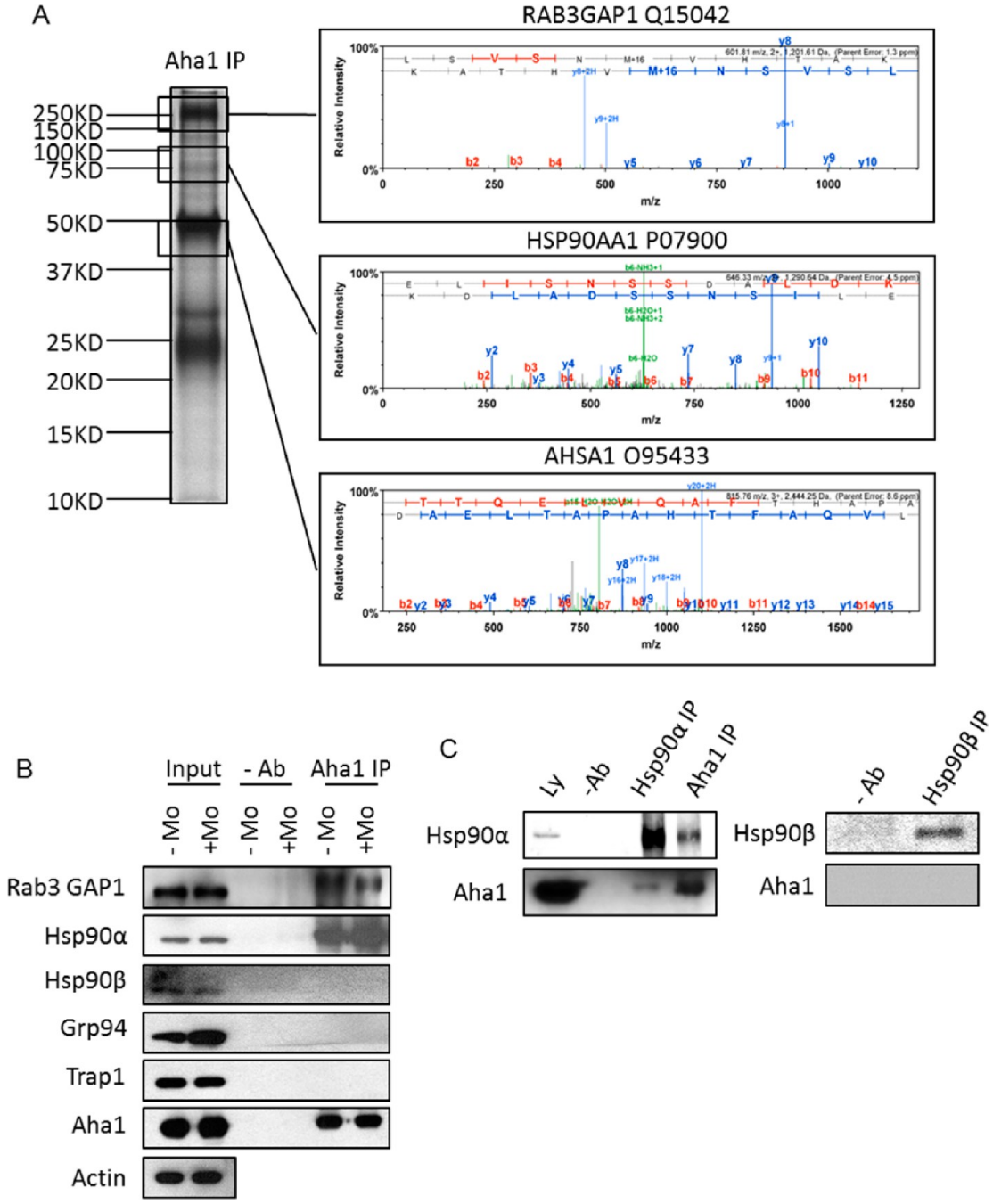

Figure 1. Aha1 binds Hsp90α and Rab3GAP1 *in vivo*. (A) Aha1 binds Hsp90α and Rab3GAP1. Aha1 was immunoprecipitated from PC3-MM2 cells, and following electrophoresis, the indicated bands were digested with trypsin and analyzed by HPLC-MS/MS. Unique peptides corresponding to Rab3GAP1, Hsp90α, and Aha1 are displayed. (B) Aha1 binds Hsp90α but no other Hsp90 isoforms. Aha1 was immunoprecipitated from PC3-MM2 cells, and Western blots were run for detecting Hsp90α, Hsp90β, Grp94, Trap1, and Aha1. Actin was used as loading control. (C) A complementary co-immunoprecipitation with Hsp90α and Hsp90β was performed in PC3-MM2 cells. Western blots were run for detecting Hsp90α, Hsp90β, and Aha1.

during different phases of the chaperone cycle to facilitate client protein maturation or degradation. N-terminal co-chaperones such as p23 (Sba1 in yeast), p50 (Cdc37 in yeast), Sgt1, and Aha1 (activator of Hsp90 ATPase) bind the N-terminal and middle domains and participate in the protein folding process. C-terminal co-chaperones such as HOP (Hsp organizing protein, Sti1 in yeast), PP5 (Ppt1 in yeast), GCUNC-45, TPR2, AIPL1, TTC4, and the peptidyl prolyl isomerase family of co-chaperones, that is, FKBP51, FKBP52, XAP2, and cyclophilin 40, also participate in the protein folding process.[18,19] Aha1 competes with HOP, p50, and p23 to stimulate the intrinsic ATPase activity of Hsp90[20,21] by binding the N-terminal and middle domains.[22,23] Aha1 is a late cofactor of the Hsp90 protein folding cycle and alters the conformation of Hsp90 to facilitate Hsp90's ATPase activity, which is critical for the folding of oncoproteins.[20] Moreover, recent studies have highlighted a role between Hsp90 and Aha1 during cell migration,[24] an important characteristic present during tumor formation and metastases.

dx.doi.org/10.1021/cb5008713 | *ACS Chem. Biol.* 2015, 10, 577−590

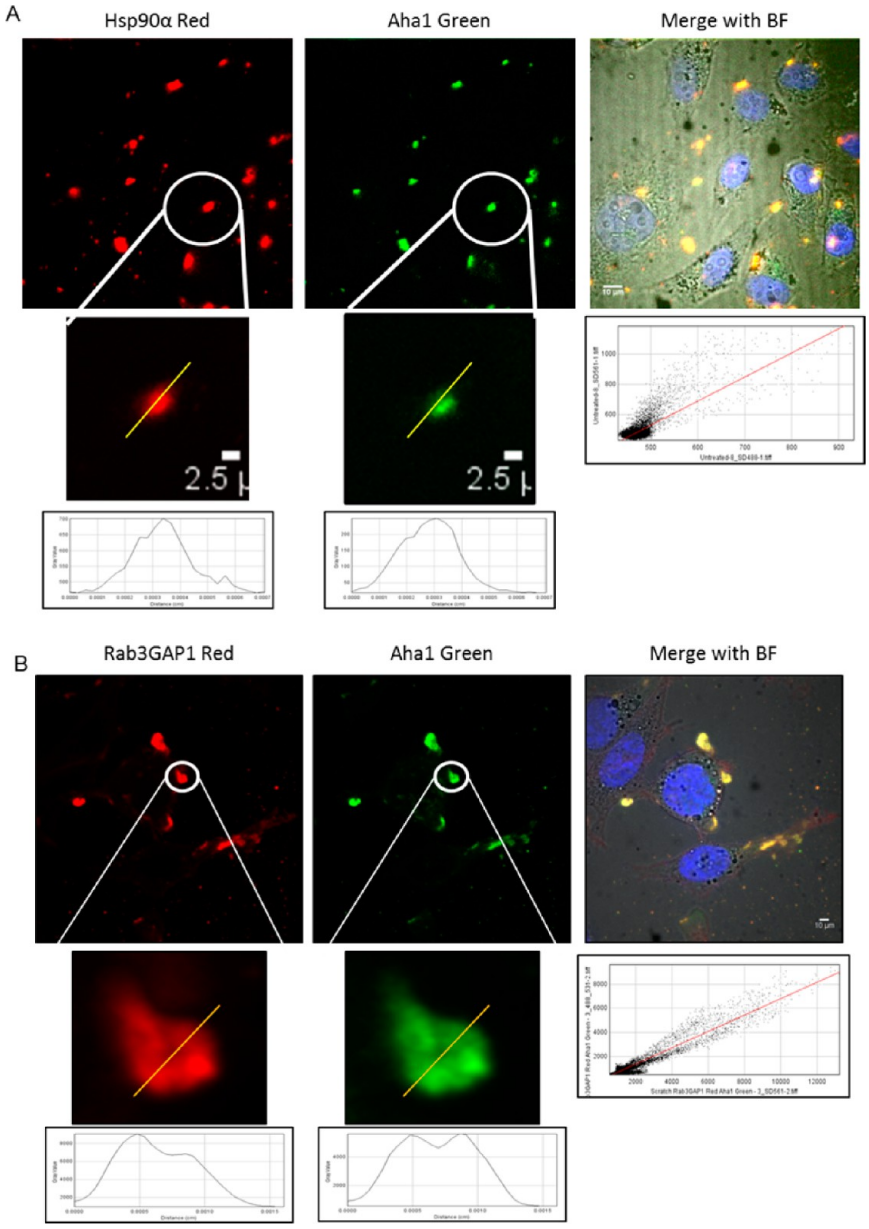

Figure 2. Aha1 colocalized with Hsp90α and Rab3GAP1 *in vivo*. (A) Colocalization of Hsp90α and Aha1. Aha1 and Hsp90α were visualized by immunofluorescence microscopy in fixed PC3-MM2 cells. Nuclei were visualized by counterstaining with DAPI. Representative photomicrographs show that Aha1−GFP and Hsp90α−RFP were colocalized as distinct foci at the polar regions of PC3-MM2 cells. The pixel intensity versus distance of each color over the drawn line is shown. (B) Co-localization of Rab3GAP1 and Aha1. Aha1 and Rab3GAP1 were visualized by immunofluorescence microscopy in fixed PC3-MM2 cells. Nuclei were visualized by counterstaining with DAPI. Representative photomicrographs show that Aha1−GFP and Rab3GAP1−RFP colocalized as distinct foci at the polar regions of PC3-MM2 cells. The pixel intensity versus distance of each color over the drawn line is shown.

In the present study, biochemical and microscopic analysis revealed that both Aha1 and Hsp90α associate with the secretory vesicle protein Rab3GAP1 and localize at the leading edge of migratory cells. Hsp90α knockdown inhibited cell migration and down-regulated Rac1, a critical component of lamellipodia and filopodia formation needed for cell migration.[25,26] Hsp90 C-terminal inhibitors were used to disrupt the interaction between Aha1 and Hsp90α, and their contribution to cell migration was explored. KU-135 and KU-174 are novobiocin-based C-terminal Hsp90 inhibitors containing a biaryl side chain that effectively disrupted the Hsp90α/Aha1 complex, caused a redistribution of the proteins throughout the cytoplasm, and inhibited cell migration. Our data provide new insights into the cellular biology of Hsp90α and support that the Hsp90α/Aha1 complex contributes to cell migration. Disruption of Hsp90α/Aha1 interactions may be a beneficial approach toward decreasing tumor metastasis.

RESULTS AND DISCUSSION

Hsp90α Associates with Aha1 and Rab3GAP1 *in Vivo*.

Previous studies have demonstrated that the binding of Aha1 to the N-terminal and middle domains of Hsp90 promotes conformational changes that stimulate Hsp90 ATPase activity.[21−23,27,28] Aha1 was co-immunoprecipitated in a low salt buffer from the PC3-MM2 cell line to determine whether Aha1 binds specific Hsp90 isoforms *in vivo*. Mass spectrometric

dx.doi.org/10.1021/cb5008713 | *ACS Chem. Biol.* 2015, 10, 577−590

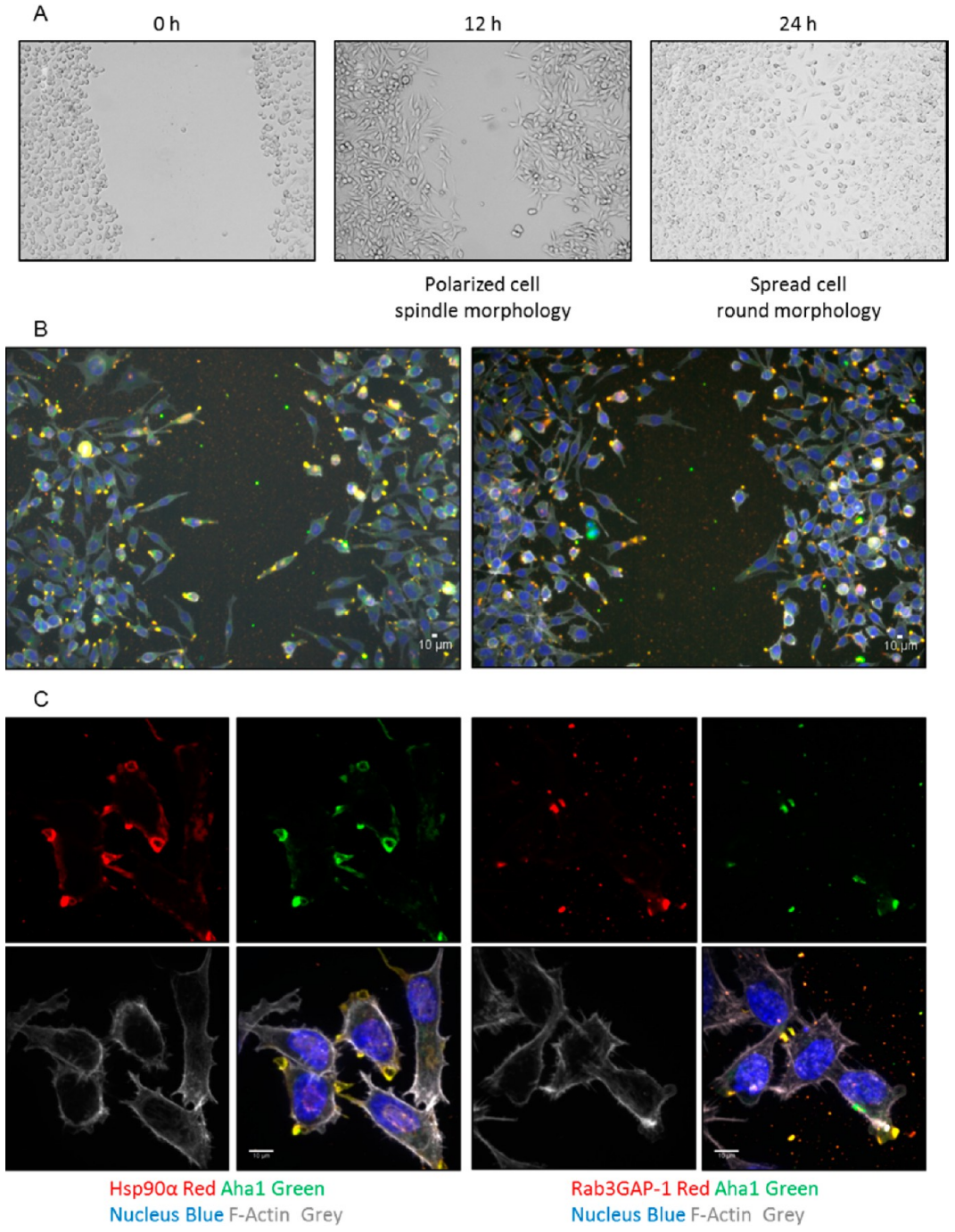

Figure 3. Co-localization of Aha1 and Hsp90α and Aha1 and Rab3GAP1 in cell migration assay. (A) Bright field photomicrographs were taken at 0, 12, and 24 h time points of the cell migration/scratch assay. At 12 h, cells at the edge of the wound are polarized or spindle shaped, but at 24 h, many cells have a round morphology. (B–C) Aha1–Hsp90α or Aha1–Rab3GAP1 were visualized by immunofluorescence microscopy in fixed PC3-MM2 cells at the 12 h time point of a cell migration assay. Representative photomicrographs show the distribution pattern of Aha1–GFP/Hsp90α–RFP and Aha1–GFP/Rab3GAP1–RFP in polarized cells at the 12 h time point. Hsp90α, Aha1, and Rab3GAP1 were localized as distinct foci at the leading edge of polarized cells. Nuclei were visualized by counterstaining with DAPI. F-actin was visualized by phalloidin (Far Red-647) and pseudocolored as gray.

analysis of the bands detected after Coomassie blue staining of the gel identified Aha1 and Rab3GAP1 associated with Hsp90α (Figure 1A). The mass spectrometric results were further verified by performing co-immunoprecipitation of proteins with Aha1 in a low salt buffer with and without molybdenum. Molybdenum is an ATP surrogate that binds the N-terminal ATP binding domain of Hsp90 and increases the ATP bound conformation of Hsp90. Since Aha1 is an ATPase activator, molybdenum stabilizes interactions between Aha1 and Hsp90α.[27] Consistent with this stabilization, more Hsp90α was co-immunoprecipitated with Aha1 in the presence of molybdenum (Figure 1B). Aha1 also pulled down Rab3GAP1 but no other Hsp90 isoforms (Figure 1B). A complementary pull down analysis was performed with Hsp90α and Hsp90β antibodies. However, only Hsp90α pulled down Aha1 (Figure 1C). Binding of Hsp90α to Aha1 was evaluated in HEK293,

dx.doi.org/10.1021/cb5008713 | ACS Chem. Biol. 2015, 10, 577–590

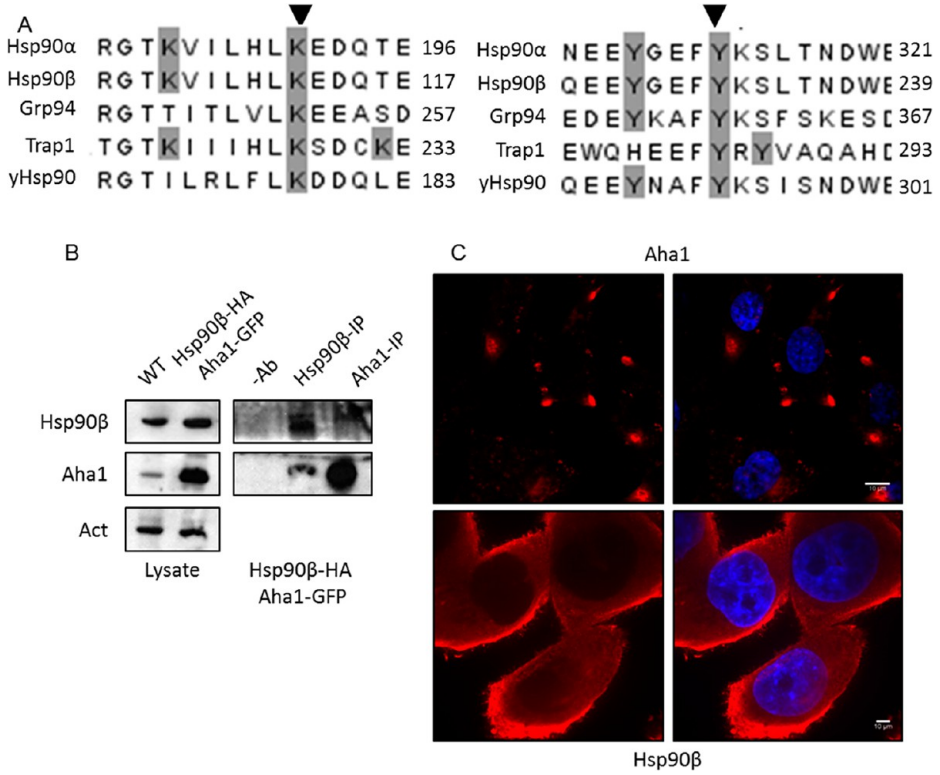

Figure 4. Aha1 binds Hsp90β during overexpression. (A) Homology alignment from Clustal W of human Hsp90 isoforms and yeast Hsp90 shows the conserved lysine and tyrosine residues that undergo SUMOylation and phosphorylation and facilitate Aha1 binding to Hsp90. (B) The Western blot was run with cell lysates from PC3-MM2 WT and transiently cotransfected with Hsp90β−HA and Aha1−GFP plasmids. Hsp90β and Aha1 were overexpressed in transfected cells and compared with nontransfected cells. Actin was loaded as control. Hsp90β and Aha1 were co-immunoprecipitated from PC3-MM2 cells that were transiently cotransfected with Hsp90β−HA and Aha1−GFP plasmids, and Western blots were performed for Hsp90β and Aha1. (C) Aha1 and Hsp90β were visualized by immunofluorescence microscopy in fixed PC3-MM2 cells. Nuclei were visualized by counterstaining with DAPI. Representative photomicrographs show that Aha1−RFP was localized as distinct foci at the edge of the cell and some throughout the cytoplasm. Hsp90β−RFP was primarily localized at the cytoplasmic membrane along with some in the cytoplasm.

50B11, HeLa, SkBr3, and MCF7 cells, and similar to the results above, Aha1 pulled down only Hsp90α, but no other Hsp90 isoform (Figure S1, Supporting Information).

Aha1 and Hsp90α Colocalize in the Secretory Vesicle. The biochemical data described above suggest that Aha1 selectively associates with Hsp90α and Rab3GAP1. Therefore, immunofluorescence microscopy was performed to support this interaction and determine its localization within the cell. Hsp90α and Aha1 were found to colocalize as distinct foci in nonmigrating cells (Figure 2A). Image quantification showed that the Pearson's coefficient (R value) was 0.70 ± 0.11 (n = 25, p < 0.001), which strongly supports Hsp90α and Aha1 colocalization and complements the co-immunoprecipitation results.

Rab3GAP1 is a GTPase activating protein of the Rab3 family and serves as a marker for secretory vesicles and exocytosis.[29] Results obtained from immunofluorescence staining suggest that Aha1 and Rab3GAP1 also colocalize (Figure 2B). Together, both colocalization data suggest that the Hsp90α/Aha1 complex is localized in secretory vesicles and may contribute to the process of exocytosis. It has been previously reported that exocytosis is polarized toward the leading edge in migrating cells.[30] As an initial step to evaluate whether the Hsp90α/Aha1 complex may play a role in cell migration and localize with Rab3GAP1 at the leading edge in migrating cells, a wound healing/scratch assay was performed. The scratch assay provides a valuable tool to evaluate cell polarity since cells at the wound edge polarize and migrate into the wound space (Figure 3A, 12 h), but upon closure of the gap, the cells no longer polarize and present a round morphology (Figure 3A, 24 h). Aha1 colocalized with both Hsp90α and Rab3GAP1 in the spindle shaped migrating cells at the leading edge of the wound (Figure 3B,C).

Hsp90β Associates with Aha1 during Overexpressing Conditions. Prior studies have identified Hsp90 residues, specifically tyrosine 313 and lysine 191, which are post-transcriptionally modified and affect Aha1 binding to Hsp90.[23,31] These two amino acid residues are conserved among all human Hsp90 isoforms, as well as yeast Hsp90 (Hsp82) (Figure 4A), and therefore other Hsp90 isoforms are likely to undergo phosphorylation and SUMOylation, respectively. However, the data presented herein suggests that Aha1 preferentially associates with Hsp90α *in vivo*. The interaction of Aha1 with other Hsp90 isoforms was investigated by the overexpression of Aha1 and Hsp90β in cells. HA tagged Hsp90β and GFP tagged Aha1 were cotransfected in PC3-MM2 cells, and then Hsp90β and Aha1 were co-immunoprecipitated. The co-immunoprecipitation results show that overexpression of Hsp90β results in Aha1 binding, suggesting that Aha1 can also bind other Hsp90 isoforms (Figure 4B).

Immunofluorescence microscopy studies revealed that Hsp90β localized to the cytoplasm and cytoplasmic membrane (Figure 4C) and that the majority of Aha1 was localized as foci at the edge of the membranes; however, a low level was

dx.doi.org/10.1021/cb5008713 | *ACS Chem. Biol.* 2015, 10, 577−590

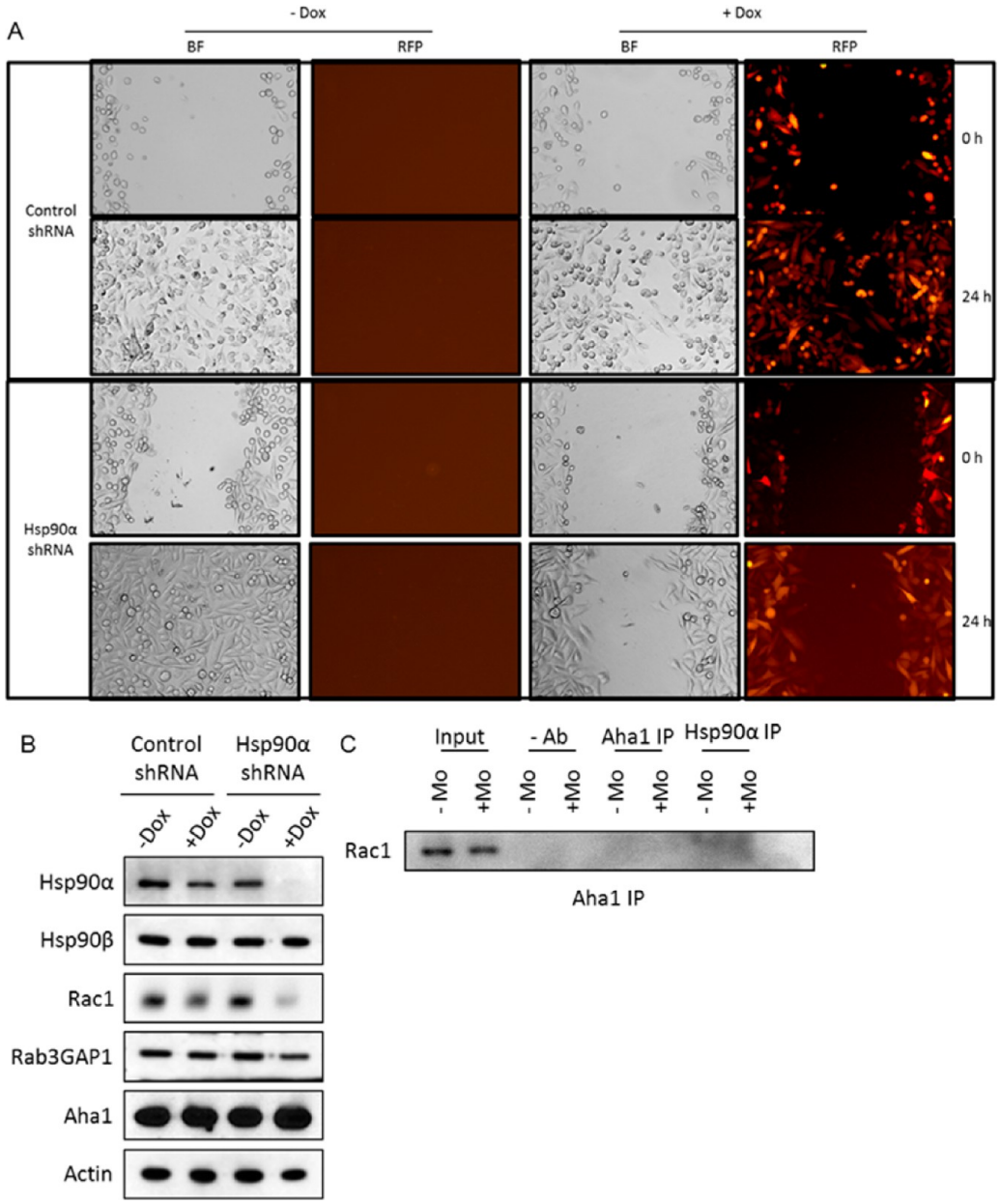

Figure 5. Hsp90α knockdown cells are defective in cell migration. (A) Cell migration assay was performed 24 h following knockdown of Hsp90α with 24 μg/mL of doxycycline (Dox). Bright field and fluorescent photomicrographs were taken at 0 and 24 h time points of the cell migration/scratch assay. (B) Hsp90α knockdown cells down-regulate Rac1. Cells were treated with doxycycline, and after 24 h, the levels of Hsp90α, Hsp90β, Rac1, Rab3GAP1, and Aha1 were analyzed by Western blotting. Actin was used as loading control.

detected within the cytoplasm (Figure 4C). This suggests that cytoplasmic Aha1 can potentially bind other Hsp90 isoforms, including Hsp90β. Several co-chaperones bind Hsp90 at various stages of the Hsp90-mediated protein folding cycle. Since Aha1 is a late phase co-chaperone, it binds the Hsp90 complex and facilitates ATP hydrolysis. Therefore, it can be expected that in the cytoplasmic pool of Hsp90β, only a relatively small amount may interact with Aha1 at any given time, which may not be detectable by co-immunoprecipitation. Consequently, the overexpression of Hsp90β and Aha1 was necessary for detection of this interaction (Figure 4B).

The significance of the Hsp90α/Aha1 complex at the leading edge of the migrating cell is 2-fold. During cancer cell migration, a large number of proteins are required for filopodia formation, focal adhesion, and translocation events.[32] These proteins are localized to the polar region of the migrating cell and require constant turnover.[5] The Hsp90α/Aha1 complex that is localized to the same region may accelerate the rate of maturation for proteins required during cell migration. Similarly, during metastasis, Hsp90α and Aha1 are secreted outside the cell to fold extracellular proteins without the use of early phase C-terminal co-chaperones. A previous report suggests that Hsp90α is post-translationally modified and that C-terminally truncated Hsp90α is secreted outside the cell and required for metastasis.[9] The current biochemical and microscopic studies further support Hsp90α secretion, since Hsp90α associates with Rab3GAP1, a protein present in secretory vesicles.[29] This study provides further evidence that Hsp90α associates with Aha1 *in vivo*, a late co-chaperone that associates with Hsp90 after the tetratricopeptide repeat (TPR) domain

dx.doi.org/10.1021/cb5008713 | *ACS Chem. Biol.* 2015, 10, 577−590

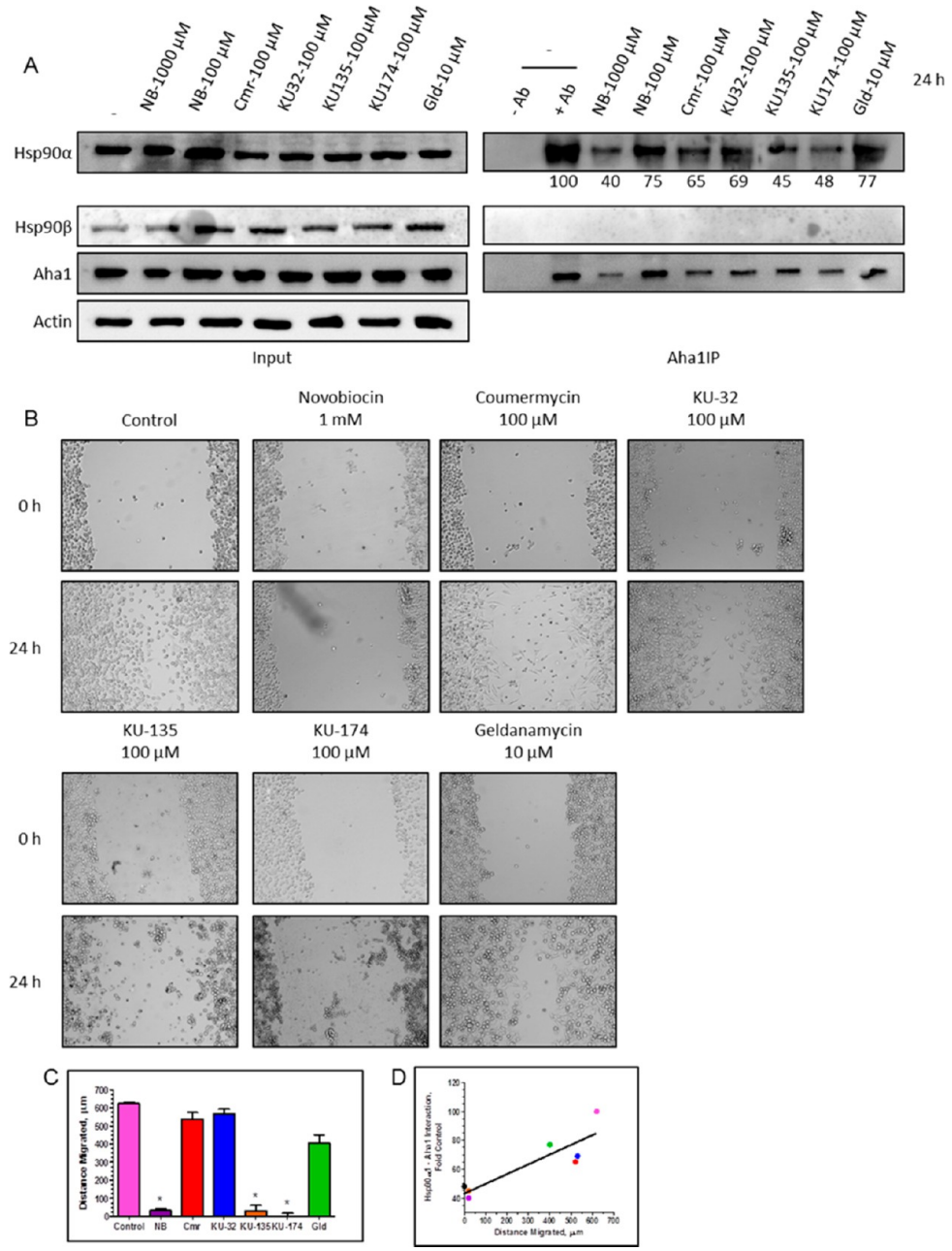

Figure 6. Hsp90 C-terminal inhibitors disrupt the Hsp90α/Aha1 complex and affect cell migration. (A) Evaluation of disruption of Aha1 and Hsp90α binding by treatment with Hsp90 terminal inhibitors. PC3-MM2 cells were treated for 24 h with DMSO (0.1%), novobiocin (1 mM or 100 μM) (NB), coumermycin (100 μM) (Cmr), KU-32 (100 μM), KU-135 (100 μM), KU-174 (100 μM), or the N-terminal inhibitor geldanamycin (10 μM) (Gld). Aha1 was immunoprecipitated, and Hsp90α, Hsp90β, and Aha1 were analyzed by Western blotting. Actin was used as loading control. Aha1 bound Hsp90α was quantified using ImageJ software and expressed as percent bound compared with the cells treated with 0.1% DMSO (control). (B) Evaluation of Hsp90 inhibitors in cell migration assay. Cell migration assay was performed with PC3-MM2 cells in the presence of DMSO (0.1%), novobiocin (1 mM), coumermycin (100 μM), KU-32 (100 μM), KU-135 (100 μM), KU-174 (100 μM), or N-terminal inhibitors geldanamycin (10 μM) for 24 h. Bright field photomicrographs were taken at 0 and 24 h time points of the cell migration/scratch assay. (C) Quantification of cell migration by PC3-MM2 cells upon treatment with the Hsp90 C-terminal inhibitors. The average distance migrated in 24 h was calculated from three independent experiments ($^*p < 0.05$). (D) The correlation between Hsp90α Aha1 interaction and cell migration. The percentage of Hsp90α bound by Aha1 was plotted against distance migrated, and the results analyzed using a linear regression ($r^2 = 0.78$).

containing co-chaperones bind the C-terminus of Hsp90α. By association with Aha1, Hsp90α may bypass the requirement of binding TPR domain containing co-chaperones, since secreted Hsp90α contains a truncated C-terminal domain, which is required for TPR-binding.[9]

Hsp90α Knockdown Inhibits Cell Migration and Down-Regulates Rac1. The data suggest that Hsp90α readily associates with Aha1 *in vivo*, colocalizes in secretory vesicles, and is potentially processed for exocytosis. Exocytosis is known to play an important role in cell migration.[30,33−35] Hsp90α was knocked down by a lentiviral-mediated shRNA to determine whether Hsp90α contributes to cell migration. The cell migration assay revealed that knockdown of Hsp90α induced a defect in cell migration (Figure 5A). Western blot data

dx.doi.org/10.1021/cb5008713 | ACS Chem. Biol. 2015, 10, 577−590

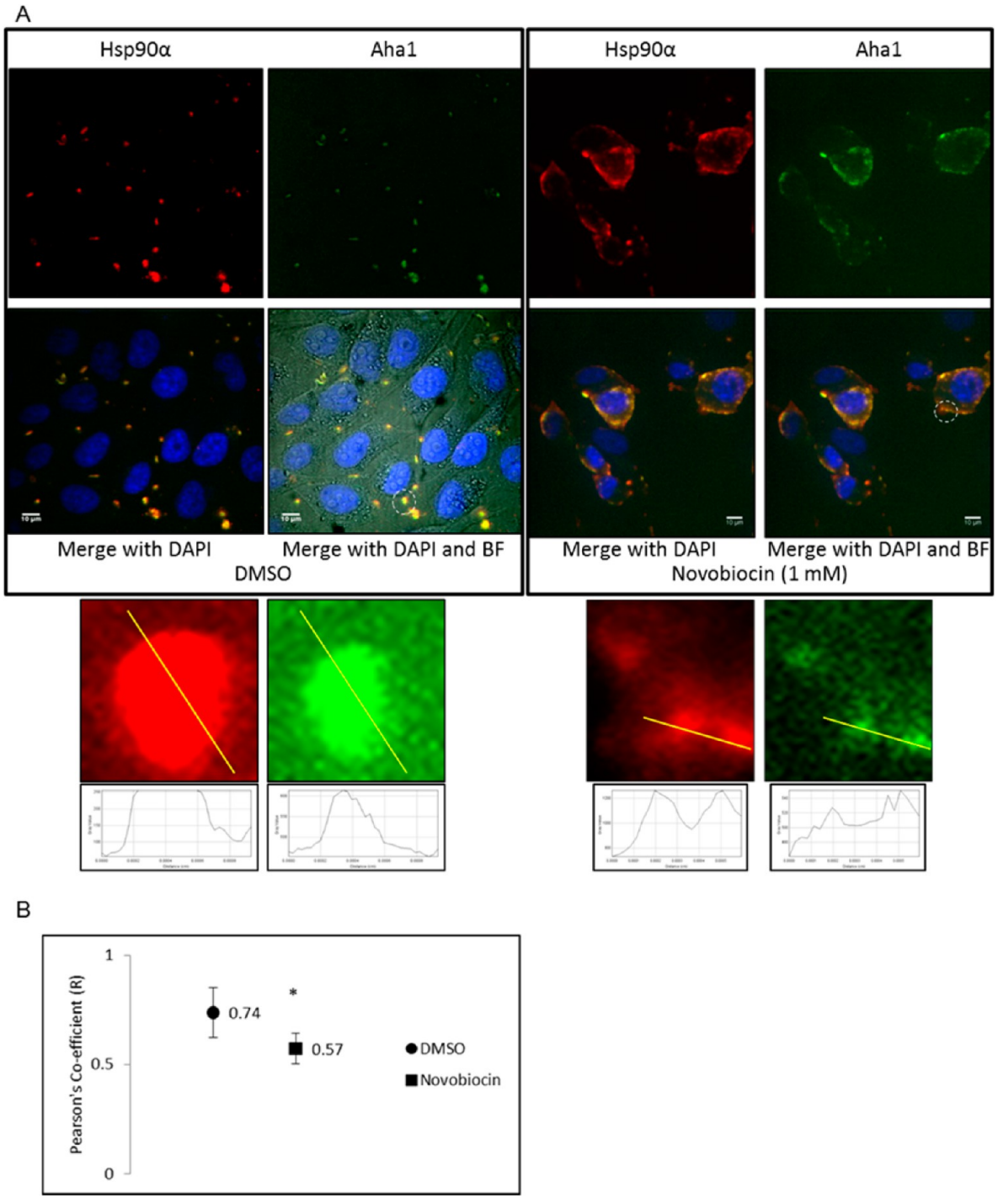

Figure 7. (A) Redistribution of Aha1 and Hsp90α in the cytoplasm. PC3-MM2 cells were treated for 24 h with 1 mM novobiocin or DMSO (0.1%). The cell were fixed and stained with Hsp90α and Aha1. Nuclei were visualized by counterstaining with DAPI. Representative photomicrographs show that Hsp90α and Aha1 were redistributed from the polar region to the cytoplasm of PC3-MM2 cells treated with novobiocin. The pixel intensity versus distance of each color over the drawn line is shown. (B) Quantification of colocalization was performed by using JACOP, and the Pearson's coefficient (R) values were calculated. The graph shows the average R values and standard deviations ($^*p < 0.05$).

revealed that Hsp90α knock down also down-regulated Rac1 (Figure 5B), a Rho family GTPase that is known to be dependent upon Hsp90[36] and regulate the actin cytoskeleton[26] and thereby cell motility. Aha1 and Hsp90α were co-immunoprecipitated and blotted for Rac1 to determine whether Hsp90α or Aha1 directly binds Rac1. However, Rac1 did not co-immunoprecipitate with either Hsp90α or Aha1 (Figure 5C).

Hsp90 C-Terminal Inhibitors Affect Cell Migration by Disrupting the Hsp90α/Aha1 Complex *in Vivo*. Prior studies by Sun and co-workers demonstrated that the Hsp90 C-terminal inhibitor novobiocin disrupted the interaction of recombinant Hsp90 and Aha1.[27] PC3-MM2 cells were incubated with DMSO, novobiocin (1 mM and 100 μM), novobiocin analogs such as KU-32 (100 μM), KU-135 (100 μM), KU-174 (100 μM), or coumermycin A1 (a novobiocin

dx.doi.org/10.1021/cb5008713 | ACS Chem. Biol. 2015, 10, 577−590

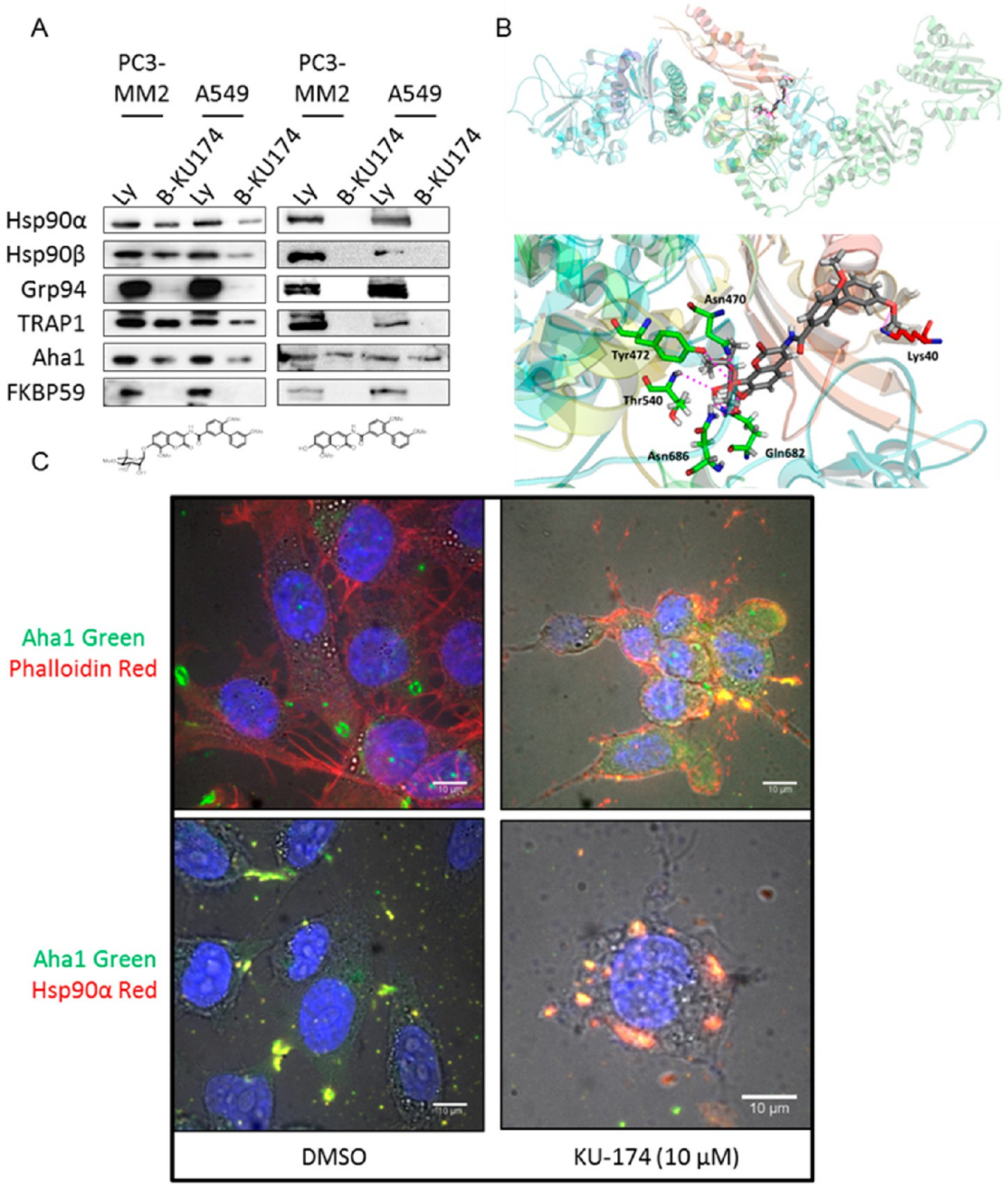

Figure 8. Hsp90 C-terminal inhibitors decrease cell migration by binding to Aha1. (A) Hsp90 C-terminal inhibitors bind all Hsp90 isoforms and Aha1. Biotinylated KU-174 and KU-174 aglycone (10 μM) were used for drug−protein interaction studies of PC3-MM2 and A549 cell lysates. Biotinylated KU-174 bound proteins were analyzed by Western blot analysis. (B) Modeled structure of the KU-174 binding site in the hHsp90α and Aha1 protein complex. (top) The hHsp90α (1−732 amino acids) homology model homodimer and the C-terminal binding site with KU-174 (black sticks) docked at the interface of two monomers (transparent blue and transparent green), as well as the Aha1 and Hsp90 crystal structure (transparent multicolored). (bottom) Close-up of KU-174 (black sticks) docked in hHsp90α (1−732 amino acids) homology model. The cross-linked fragment and predicted hydrogen bonds (dashes) are depicted in magenta. One molecule of KU-174 is shown to be bound to Hsp90 homodimer and Aha1 monomer. (C) Mislocalization of the Hsp90α/Aha1 complex in KU-174 treated cells. PC3-MM2 cells were treated for 24 h with 10 μM KU-174 or DMSO (0.1%). The cells were fixed and stained with phalloidin and Aha1 or Hsp90α and Aha1. Nuclei were visualized by counterstaining with DAPI. F-actin was visualized by phalloidin (Red-555). Representative photomicrographs show that Hsp90α and Aha1 were redistributed from the polar region to the cytoplasm of PC3-MM2 cells treated with KU-174.

dimer, 100 μM), or an unrelated N-terminal inhibitor, geldanamycin (100 μM) to identify structure−function relationships involved with the dissociation of Hsp90α and Aha1 (Figure 6A). The concentration of Hsp90 inhibitors were chosen based on antiproliferative values manifested by these compounds against the PC3-MM2 cell line.[37−39] In cells treated with 1 mM or 100 μM novobiocin, the amount of Hsp90α that co-immunoprecipitated with Aha1 was ∼40% and ∼75% of that observed in cells receiving DMSO, respectively (Figure 6A). Similarly, in cells treated with KU-135 and KU-174, ∼45% and ∼48% of Hsp90α co-immunoprecipitated with Aha1 compared with the control, respectively. Among the

dx.doi.org/10.1021/cb5008713 | ACS Chem. Biol. 2015, 10, 577−590

Hsp90 C-terminal inhibitors, KU-32 (100 μM), and coumermycin A1 (100 μM) were the least effective at disrupting the Hsp90α/Aha1 complex and pulled down ~69% and ~65% Hsp90α, respectively. Similarly, Hsp90α and Aha1 interactions were less sensitive to disruption by the Hsp90 N-terminal inhibitor, geldanamycin (10 μM). It is unlikely that this lack of dissociation is due to the lower concentration of geldanamycin, since higher concentrations promote cell death.

Cell migration assays were conducted to determine whether disrupting Hsp90α and Aha1 binding by Hsp90 inhibitors has a functional effect consistent with Hsp90α down-regulation. A strong correlation ($r^2 = 0.78$) existed between the efficacy of C-terminal inhibitors at disrupting Hsp90α/Aha1 association and a decrease in migration (Figure 6B–D). Among the compounds tested, novobiocin, KU-135, and KU-174 were most effective (Figure 6B and Figure S2, Supporting Information). In fact, at all concentrations tested, cells treated with novobiocin, KU-135 and KU-174 exhibited a round morphology, instead of the polarized/spindle shaped morphology needed for migration (Figure 6B and Figure S2, Supporting Information). Additional cell migration studies were conducted with KU-174 to determine whether the inhibition of cell migration was due to inhibition of cell growth. The results show that even at 500 nM concentration, KU-174 inhibited cell migration, which is 10-fold lower than the IC_{50} value (Figure S3, Supporting Information). KU-32, coumermycin, and geldanamycin did not exhibit substantial antimigratory activity, which correlated with less disruption of the Hsp90α/Aha1 complex. Overall, these data support a structure–function relationship in the ability of novobiocin-based C-terminal Hsp90 inhibitors to disrupt Hsp90α/Aha1 interactions.

Novobiocin Redistributes Hsp90α/Aha1 to the Cytoplasm *in Vivo*. Immunofluorescence microscopy was performed in PC3-MM2 cells incubated with novobiocin (1 mM, 0.1% DMSO) or with DMSO (0.1%) for 24 h to determine whether Hsp90 inhibitors can disrupt binding between Hsp90α and Aha1. Novobiocin treatment partially disrupted Hsp90α/Aha1 interactions (Figure 7A) and altered their cellular colocalization (r =0.57 ± 0.18, $p < 0.001$, $n = 25$), compared with DMSO (0.1%) treated (r = 0.74 ± 0.07, $p < 0.001$, $n = 25$) cells (Figure 7B). The degree of disruption of the Hsp90α/Aha1 complex in the novobiocin treated cells was found to be similar in both the co-immunoprecipitation-based biochemical method (Figure 6A) and the immunofluorescence-based microscopic method (Figure 7).

Furthermore, it was observed that novobiocin prevented Hsp90α and Aha1 from localizing to the polar region, as both were redistributed to the cytoplasm and cytoplasmic membranes (Figure 7B). Redistribution of the Hsp90α/Aha1 complex is particularly important for explaining the fact that novobiocin either disrupts cell polarity or prevents localization of Hsp90α in the polar region. In either case, Hsp90α may affect maturation of the client protein, Rac1, which is critical for cell migration.

Hsp90 C-Terminal Inhibitor KU174 Disrupts the Hsp90α/Aha1 Complex by Binding Aha1. Hsp90 contains four structural domains; a highly conserved 25 kDa N-terminal domain, a charged linker region that connects the N-terminus with the ~40 kDa middle domain that binds to substrates and partner proteins, and a 12 kDa C-terminal dimerization domain. The conserved N-terminal domain contains an ATP-binding pocket with a lid that is open during ADP binding but is closed when bound to ATP. Thus, binding to ATP or ADP produces a conformational change that enables the N-terminal domain to become accessible for client protein binding. The middle domain contains a region to which the γ-phosphate of ATP binds in the closed conformation. Binding of Aha1 to the N-terminal and middle domains of Hsp90 promotes conformational changes that stimulate Hsp90 ATPase activity.[21−23,27,28] In addition, the C-terminal domain possesses a nucleotide-binding site that appears to exhibit allosteric control over the N-terminal ATP-binding site and may serve to elicit opening of the Hsp90 homodimer. The crystal structure of human and yeast Hsp90 has been solved and discussed in many reviews. However, the cocrystal structure of inhibitors bound to the C-terminus has not been elucidated.[19,40,41] Both the N- and C-terminal nucleotide binding sites have been targeted for the development of anticancer agents that inhibit the Hsp90-mediated protein folding machinery.[42,43] One characteristic shared by Hsp90 C-terminal inhibitors that contain an aryl amide side chain is that they do not induce the heat shock response. However, they do induce the degradation of Hsp90-dependent client proteins and cell death.

Biotinylated KU-174, a potent Hsp90 C-terminal inhibitor, was used for drug–protein binding assays to determine how the C-terminal inhibitors disrupted Hsp90α/Aha1 interactions. Biotinylated KU-174 bound all four Hsp90 isoforms along with Aha1 but not the C-terminal co-chaperone FKBP59 (Figure 8A). Binding analysis with the biotinylated KU-174 aglycone revealed the noviose to be required for binding to Hsp90 (Figure 8A), and this confirms previously published observations.[37] Notably, biotinylated KU-174 aglycone did not bind any of the Hsp90 isoforms but did interact with Aha1.

Previous studies have shown that the novobiocin analog KU-174 exhibits selective activity against the prostate cancer cell line PC3-MM2 compared with normal human renal proximal tubule epithelial cells (RPTEC). KU-174 was also shown to reduce the size of tumors *in vivo* using a rat PC3-MM2 xenograft tumor model.[37] In those studies, it was shown that KU-174 specifically binds Hsp90. In the present study, it was observed that the noviose sugar moiety on KU-174 provides strong affinity for Hsp90 and that an aryl amide side chain is important for binding Aha1. Indeed, an acetamide substitution (KU-32) in lieu of the biaryl side chain did not disrupt Aha1 binding to Hsp90α (Figure 5A) and did not affect cell migration (Figure 5B and Figure S2, Supporting Information).

Recently, a homology model of hHsp90α (732 amino acids) was elucidated via photoaffinity and molecular modeling studies.[44] KU-174 was docked into the Hsp90 C-terminal homology model, onto which the crystal structure of Aha1–Hsp90 (PDB 1USU)[45] was overlaid to determine whether Hsp90 inhibitors can disrupt binding between Hsp90α and Aha1 (Figure 8B). As shown in Figure 8B, the noviose sugar of KU-174 forms important interactions with several amino acids (Thr540, Gln682, and Asn686), while the methoxy of the coumarin core exhibits hydrogen-bonding interactions with Asn470 and Tyr472, indicating a strong affinity of KU-174 for Hsp90. Interestingly, the 3′-OMe of the biaryl side chain appears to form a key hydrogen-bonding interaction with Lys40 of Aha1, which may account for its binding. Thus, in accord with the affinity studies, docking studies suggest that KU-174 exhibits strong affinity for both Hsp90 and Aha1. In contrast, the KU-174 aglycone has little to no affinity for Hsp90, but can still interact with Aha1 via its biaryl side chain. Collectively, these data suggest that the methoxylated biaryl side chain

dx.doi.org/10.1021/cb5008713 | ACS Chem. Biol. 2015, 10, 577–590

present on the KU-174 and KU-135 Hsp90 C-terminal inhibitors are required for Aha1 binding and are responsible for disrupting the Hsp90α/Aha1 complex, which inhibits cell migration. Consistent with this hypothesis, KU-32 does not contain a biaryl side chain and was not effective at disrupting Hsp90α/Aha1 interactions and, therefore, did not significantly inhibit cell migration (Figure 6).

Immunofluorescence analysis of KU-174 treated cells showed round cell morphology and the presence of F-actin patches at the cortex (Figure 8C). KU-174 treated cells formed filopodia, suggesting that Hsp90 C-terminal inhibitors or the Hsp90α/Aha1 complex does not affect initial formation of filopodia. On the other hand, DMSO treated cells exhibited a spindle-shaped morphology characterized by F-actin along the boundary of the cell (Figure 8C). This suggests that KU-174 disrupts Hsp90α/Aha1 interactions and results in a loss of cell polarity without affecting initial filopodia formation. Neither KU-174 treated cells nor Hsp90α knock down cells were defective in filopodia formation, suggesting that Cdc42, which is required for filopodia formation,[26] is not dependent upon Hsp90α.

Biotinylated KU-174 binds the C-terminal region of all Hsp90 isoforms. The aryl amide side chain of KU-174 is required for Aha1 binding and provides the antimigratory activity manifested by these compounds. Since Hsp90 C-terminal inhibitors also bind other Hsp90 isoforms (Figure 8A), it is likely that these compounds have other anticancer activities in addition to inhibiting cell migration.[37,39,46] However, specifically targeting the Hsp90α/Aha1 complex may result in the inhibition of cell migration, one of the early phases of metastasis. This is particularly useful for the development of new drugs for the treatment of prostate and breast cancers, which can be removed by surgery but often metastasize and reappear at distant sites. This study provides evidence that it may be possible to develop an inhibitor of the Hsp90α/Aha1 complex that can be used to regulate cell migration without broad cytotoxicity.

Previous reports indicate a role for Hsp90α in metastases and stress resistance.[8,10,11,47] For the first time, we show that Hsp90α readily associates with the co-chaperone Aha1, localizes to secretory vesicles, and plays a role in cell migration. Hsp90α knock down cells were defective in cell migration, and this was associated with the down-regulation of Rac1. The Hsp90 C-terminal inhibitors, including novobiocin and select analogs, inhibited cell migration by disrupting Hsp90α/Aha1 interactions, promoted a loss of cell polarity as indicated by formation of rounded cell morphology and loss of F-actin organization, and caused a defect in cell migration. The identification of specific structural aspects of novobiocin-based Hsp90 C-terminal inhibitors that selectively disrupt the Hsp90α/Aha1 complex provides a novel approach to inhibit cell migration. Future research will be aimed at developing improved analogs that completely disrupt interactions between Hsp90α and Aha1. In conclusion, we propose that Hsp90α does not go through the elaborate chaperone cycle like other Hsp90 isoforms but instead binds Aha1 directly during cell migration to fold client proteins necessary for this function.

METHODS

Chemicals, Reagents, and Plasmids. Novobiocin analogues were synthesized as previously described. Novobiocin, coumermycin, KU-32, KU-135, KU-174, and geldanamycin were dissolved in DMSO and stored at −20 °C until use. Aha1-GFP plasmid was obtained from Origene (Catalog # RG201782), and Hsp90β-HA plasmid was a kind donation from Dr. Jeff Staudinger. The plasmids were transfected in PC3-MM2 cell line by lipofectamine 2000 protocol.

Antibodies. The following antibodies were used for Western blotting and/or co-immunoprecipitation: rabbit anti-Hsp90α (Neomarkers, RB-119-P), goat anti-Hsp90β (SantaCruz), rat anti-Grp94 (SantaCruz), mouse anti-Trap1(BD Biosciences), rabbit anti-Aha1 (Abcam), mouse anti-Aha1 (Abcam), rabbit anti-Actin (SantaCruz), mouse anti-Fkbp59 (Stressgen), Rabbit Rab3GAP1 (Sigma), Mouse Rac (Abcam, detects Rac1 with slight cross reactivity with Rac2), Phalloidin 555 (Invitrogen), and Phalloidin 647 (Invitrogen).

Cell Lines. The HEK293, HeLa, SkBr3, MCF7 and PC3-MM2 cell lines were maintained in DMEM supplemented with 10% FBS, streptomycin, and penicillin at 37 °C, 5% CO_2. 50B11 cells were maintained in DMEM supplemented with 10% FBS, blasticidin (5 μg/mL), streptomycin, and penicillin at 37 °C, 5% CO_2. Lung cancer A549 cells were maintained in ATCC-formulated F-12K media supplemented with 10% FBS, streptomycin and penicillin. Inducible knockdown of Hsp90α in the PC3-MM2 cell line was accomplished using a tetracycline inducible shRNA construct containing a hairpin sequence specific for the Hsp90α isoform reported earlier.[48] The stable, transduced control shRNA and Hsp90α knockdown cells were cultured as above but with the addition of 2.5 μg/mL puromycin. Induction of shRNA expression with tetracycline was monitored by the increase in TurboRFP fluorescence which is driven by the tetracycline response element (TRE) for Hsp90α. shRNA expression was induced with the addition of 1−24 μg/mL doxycycline.

Western Blot Analysis. The various cell lines were harvested in cold PBS and lysed in mammalian protein extraction reagent (MPER, Pierce) lysis buffer containing protease and phosphatase inhibitor cocktails (Roche) on ice for 1 h. Cancer patients' tissue samples were homogenized and lysed in Native Blue buffer containing protease and phosphatase inhibitor cocktails (Roche) on ice for 1h. Lysates were clarified at 14,000g for 10 min at 4 °C. Protein concentrations were determined using the Pierce BCA protein assay kit per the manufacturer's instructions. Equal amounts of protein (2.5−20 μg) were electrophoresed under reducing conditions (8% polyacrylamide gel), transferred to a polyvinylidene fluoride membrane (PVDF), and immunoblotted with the corresponding specific antibodies. Membranes were incubated with an appropriate horseradish peroxidase-labeled secondary antibody, developed with a chemiluminescent substrate, and visualized.

Co-immunoprecipitation. PC3-MM2 cell lines were plated in 10 cm cell culture dishes or T25 flasks and allowed to grow to ∼80% confluency. PC3-MM2 cell lines were untreated, or received DMSO (0.1%), or the indicated drugs dissolved in DMSO. After drug treatments PC3-MM2 cell lines were harvested in lysis buffer containing 0.1% NP40, 50 mM Tris (pH 7.5), 150 mM NaCl, with or without 20 mM MoO_4, protease and phosphatase inhibitor cocktails (Roche). Lysates were clarified and protein concentration was determined using BCA assay. For co-immunoprecipitation, 500 μg of total protein was diluted to 500 μL total volume in lysis buffer and incubated with 10 μL of primary antibody overnight at 4 °C with rocking. Immune complexes were captured with 30 μL of DynaBeads Protein G (Invitrogen) for 3 h with rocking at 4 °C. Protein G Bead complexes were washed three times with lysis buffer and eluted with sample buffer. Samples were then boiled and subjected to SDS−PAGE and Western blot analysis.

Mass Spectrometry and Protein Identification. For co-immunoprecipitation based mass spectrometry analysis, 4 mg of total protein was diluted to 500 μL total volume in lysis buffer and incubated with 15 μL of primary antibody overnight at 4 °C with rocking. Immune complexes were captured with 35 μL of DynaBeads Protein G (Invitrogen) for 3 h with rocking at 4 °C. Protein G Bead complexes were washed three times with lysis buffer and eluted with sample buffer. Samples were then boiled and subjected to SDS−PAGE and an aliquot used for Western blot analysis. The gel was stained with GelCode Blue Stain Reagent (Pierce) overnight and destained with water. The stained portions of the gels were cut for in-gel tryptic digestion, the eluates were introduced into the LTQ-FT tandem mass

spectrometer (ThermoFinnigan, Waltham, MA), and mass spectra were acquired in the positive ion mode as described previously.[49]

Drug−Protein Interaction Assay. PC3-MM2 and A549 cell lines were harvested in lysis buffer containing 0.1% NP40, 50 mM Tris (pH 7.5), 150 mM NaCl, protease and phosphatase inhibitor cocktails (Roche). The cell lysates (200 μg) were incubated with biotinylated KU-174 (10 μM) or biotinylated KU-174 aglycone overnight at 4 °C with rocking. Drug−protein complexes were captured with 30 μL of Streptavidin DynaBeads (Invitrogen) for 3 h with rocking at 4 °C. Streptavidin bead complexes were washed three times with lysis buffer and eluted with sample buffer. Samples were then boiled and subjected to SDS−PAGE and Western blot analysis.

Molecular Modeling. Docking studies were performed using Surflex-Dock in Sybyl v8.0. A homology model of hHsp90α based on the open HtpG SAXS structure was used as the receptor, while the protomol was generated using docked novobiocin.[44] The energy minimized molecules were docked with 10 different starting conformations with ring flexibility allowed. Crystal structure of Aha1-Hsp90 (PDB: 1USU)[45] was then overlaid on the homology model of hHsp90α. Pymol was used for visual interpretation and figure preparation.

Immunofluorescence Analysis. For the imaging, 1 μm-Slide 8 well ibidiTreat IBIDI glass slides were used. PC3-MM2 cells were fixed with freshly made 4% (w/w) paraformaldehyde in PBS for 15 min, permeabilized with 0.1% (w/w) Tween 20 in PBS for 5 min and quenched with 0.1% (w/w) sodium borohydride for 5 min. The sections were, blocked with 3% (w/w) BSA in PBS for 1 h, incubated with the primary antibody at a 1:100 concentration in 1% BSA in PBS overnight, prior to incubation with secondary antibody conjugated with Alexa Fluor 488 or 568 for 3 h. The sections were counterstained with DAPI and/or with Phalloidin to visualize DNA and F-Actin, respectively. The wells were washed with PBS three times after each step. Confocal images were acquired using a custom epifluorescent/confocal microscope composed of the following components: an Olympus IX81 inverted spinning disc confocal microscope base (Olympus America, Center Valley, PA), a Prior microscope stage for automated image acquisition (Prior Scientific, Rockland, MA), an Olympus 40X Long Working Distance Air objective for epifluorescence images (Olympus), an Olympus 60X oil Immersion objective for confocal images (Olympus) and a Hamamatsu Electron Multiplying Charge-Coupled Device (EMCCD) camera (Hamamatsu, Hamamatsu, Shizuoka Prefecture, Japan). Images were captured using the acquisition and analysis software, SlideBook (Intelligent Imaging Innovations (3i), Denver, CO). Images were collected with 8−10 image stacks with a 0.3 μm step size through the cells. Images were processed using ImageJ software (NIH).

Densitometry and Statistical Analysis. Western blot films were digitally captured using a standard flatbed scanner. The digital blots were then converted to 16-bit black and white images using ImageJ software. Densitometric measurements were then performed in ImageJ using the "Gels" tool. Peak areas were used as a measure of protein levels. Statistical analysis was performed using Microsoft Excel; statistical significance was determined using a paired, two-tailed *t* test or a Mann−Whitney test to determine statistical significance of nonparametric data. For colocalization studies Just Another Colocalization Plugin (JACoP) was installed and the Pearson's coefficient (R) were measured.

Cell migration Assay. The cells were seeded in a 24-well plate in complete media and allowed to form a monolayer. After monolayer formation, the scratch was introduced with the help of a sterile 0.1−10 μL pipet tip. The media was replaced with fresh media in the absence or presence of the indicated drug concentrations. Photomicrographs were taken at different time points with an Olympus IX71 microscope using 10x air lens with CellSans Dimensions software. The images were processed with ImageJ software. The average horizontal distance between the scratches were measured at various time points. The migration distance at a particular time point was calculated as [(length of scratch at 0 time point - length of scratch at that time point)/2]. The statistical analysis was done in Excel and statistical significance was calculated on three independent experiments.

■ ASSOCIATED CONTENT

Supporting Information

Comparison of Aha1 binding with different Hsp90 isoforms, inhibition fo cell migration by Hsp90 C-terminal inhibitors, and inhibition of cell migration by KU-174. This material is available free of charge via the Internet at http://pubs.acs.org.

■ AUTHOR INFORMATION

Corresponding Author

*Brian S. J. Blagg. E-mail: bblagg@ku.edu.

Notes

The authors declare no competing financial interest.

■ ACKNOWLEDGMENTS

The authors thank N. Anatolyevna-Galeva at the University of Kansas Mass Spectrometry and Analytical Proteomics Laboratory for assisting in the proteomic analysis. We thank J. Staudinger (The University of Kansas, Pharmacology and Toxicology Department) for providing the Hsp90β-HA plasmid that was originated in W. Sessa's laboratory (Yale University School of Medicine). We thank H. Zhao and K. B. Reddy of the Blagg group for providing KU-32, KU-135, and KU-174. This work was supported by Grants CA109265 to B.S.J.B. and DK095911 to R.T.D. from The National Institutes of Health.

■ REFERENCES

(1) Small, J. V., Stradal, T., Vignal, E., and Rottner, K. (2002) The lamellipodium: Where motility begins. *Trends Cell Biol. 12*, 112−120.
(2) Machesky, L. M. (2008) Lamellipodia and filopodia in metastasis and invasion. *FEBS Lett. 582*, 2102−2111.
(3) Hall, A. (1998) Rho GTPases and the actin cytoskeleton. *Science 279*, 509−514.
(4) Mattila, P. K., and Lappalainen, P. (2008) Filopodia: Molecular architecture and cellular functions. *Nat. Rev. Mol. Cell Biol. 9*, 446−454.
(5) Palamidessi, A., Frittoli, E., Ducano, N., Offenhauser, N., Sigismund, S., Kajiho, H., Parazzoli, D., Oldani, A., Gobbi, M., Serini, G., Di Fiore, P. P., Scita, G., and Lanzetti, L. (2013) The GTPase-activating protein RN-tre controls focal adhesion turnover and cell migration. *Curr. Biol. 23*, 2355−2364.
(6) Sahu, D., Zhao, Z., Tsen, F., Cheng, C. F., Park, R., Situ, A. J., Dai, J., Eginli, A., Shams, S., Chen, M., Ulmer, T. S., Conti, P., Woodley, D. T., and Li, W. (2012) A potentially common peptide target in secreted heat shock protein-90alpha for hypoxia-inducible factor-1alpha-positive tumors. *Mol. Biol. Cell 23*, 602−613.
(7) Li, W., Sahu, D., and Tsen, F. (2012) Secreted heat shock protein-90 (Hsp90) in wound healing and cancer. *Biochim. Biophys. Acta 1823*, 730−741.
(8) Eustace, B. K., Sakurai, T., Stewart, J. K., Yimlamai, D., Unger, C., Zehetmeier, C., Lain, B., Torella, C., Henning, S. W., Beste, G., Scroggins, B. T., Neckers, L., Ilag, L. L., and Jay, D. G. (2004) Functional proteomic screens reveal an essential extracellular role for hsp90 alpha in cancer cell invasiveness. *Nat. Cell Biol. 6*, 507−514.
(9) Wang, X., Song, X., Zhuo, W., Fu, Y., Shi, H., Liang, Y., Tong, M., Chang, G., and Luo, Y. (2009) The regulatory mechanism of Hsp90alpha secretion and its function in tumor malignancy. *Proc. Natl. Acad. Sci. U. S. A. 106*, 21288−21293.
(10) Chen, J. S., Hsu, Y. M., Chen, C. C., Chen, L. L., Lee, C. C., and Huang, T. S. (2010) Secreted heat shock protein 90alpha induces colorectal cancer cell invasion through CD91/LRP-1 and NF-kappaB-mediated integrin alphaV expression. *J. Biol. Chem. 285*, 25458−25466.
(11) Solier, S., Kohn, K. W., Scroggins, B., Xu, W., Trepel, J., Neckers, L., and Pommier, Y. (2012) Heat shock protein 90alpha (HSP90alpha), a substrate and chaperone of DNA-PK necessary for the apoptotic response. *Proc. Natl. Acad. Sci. U. S. A. 109*, 12866−12872.

(12) Sreedhar, A. S., Kalmar, E., Csermely, P., and Shen, Y. F. (2004) Hsp90 isoforms: Functions, expression and clinical importance. *FEBS Lett. 562*, 11−15.
(13) Luo, B., Lam, B. S., Lee, S. H., Wey, S., Zhou, H., Wang, M., Chen, S. Y., Adams, G. B., and Lee, A. S. (2011) The endoplasmic reticulum chaperone protein GRP94 is required for maintaining hematopoietic stem cell interactions with the adult bone marrow niche. *PloS one. 6*, No. e20364.
(14) Ni, M., and Lee, A. S. (2007) ER chaperones in mammalian development and human diseases. *FEBS Lett. 581*, 3641−3651.
(15) Felts, S. J., Owen, B. A., Nguyen, P., Trepel, J., Donner, D. B., and Toft, D. O. (2000) The hsp90-related protein TRAP1 is a mitochondrial protein with distinct functional properties. *J. Biol. Chem. 275*, 3305−3312.
(16) Hua, G., Zhang, Q., and Fan, Z. (2007) Heat shock protein 75 (TRAP1) antagonizes reactive oxygen species generation and protects cells from granzyme M-mediated apoptosis. *J. Biol. Chem. 282*, 20553−20560.
(17) Trepel, J., Mollapour, M., Giaccone, G., and Neckers, L. (2010) Targeting the dynamic HSP90 complex in cancer. *Nat. Rev. Cancer 10*, 537−549.
(18) Li, J., Richter, K., and Buchner, J. (2011) Mixed Hsp90-cochaperone complexes are important for the progression of the reaction cycle. *Nat. Struct Mol. Biol. 18*, 61−66.
(19) Pearl, L. H., and Prodromou, C. (2006) Structure and mechanism of the Hsp90 molecular chaperone machinery. *Annu. Rev. Biochem. 75*, 271−294.
(20) Harst, A., Lin, H., and Obermann, W. M. (2005) Aha1 competes with Hop, p50 and p23 for binding to the molecular chaperone Hsp90 and contributes to kinase and hormone receptor activation. *Biochem. J. 387*, 789−796.
(21) Panaretou, B., Siligardi, G., Meyer, P., Maloney, A., Sullivan, J. K., Singh, S., Millson, S. H., Clarke, P. A., Naaby-Hansen, S., Stein, R., Cramer, R., Mollapour, M., Workman, P., Piper, P. W., Pearl, L. H., and Prodromou, C. (2002) Activation of the ATPase activity of hsp90 by the stress-regulated cochaperone aha1. *Mol. Cell 10*, 1307−1318.
(22) Lotz, G. P., Lin, H., Harst, A., and Obermann, W. M. (2003) Aha1 binds to the middle domain of Hsp90, contributes to client protein activation, and stimulates the ATPase activity of the molecular chaperone. *J. Biol. Chem. 278*, 17228−17235.
(23) Mollapour, M., Bourboulia, D., Beebe, K., Woodford, M. R., Polier, S., Hoang, A., Chelluri, R., Li, Y., Guo, A., Lee, M. J., Fotooh-Abadi, E., Khan, S., Prince, T., Miyajima, N., Yoshida, S., Tsutsumi, S., Xu, W., Panaretou, B., Stetler-Stevenson, W. G., Bratslavsky, G., Trepel, J. B., Prodromou, C., and Neckers, L. (2014) Asymmetric Hsp90 N domain SUMOylation recruits Aha1 and ATP-competitive inhibitors. *Mol. Cell 53*, 317−329.
(24) Desjardins, F., Delisle, C., and Gratton, J. P. (2012) Modulation of the cochaperone AHA1 regulates heat-shock protein 90 and endothelial NO synthase activation by vascular endothelial growth factor. *Arterioscler., Thromb., Vasc. Biol. 32*, 2484−2492.
(25) Heasman, S. J., and Ridley, A. J. (2008) Mammalian Rho GTPases: New insights into their functions from in vivo studies. *Nat. Rev. Mol. Cell Biol. 9*, 690−701.
(26) Hall, A. (1994) Small GTP-binding proteins and the regulation of the actin cytoskeleton. *Annu. Rev. Cell Biol. 10*, 31−54.
(27) Sun, L., Prince, T., Manjarrez, J. R., Scroggins, B. T., and Matts, R. L. (2012) Characterization of the interaction of Aha1 with components of the Hsp90 chaperone machine and client proteins. *Biochim. Biophys. Acta 1823*, 1092−1101.
(28) Meyer, P., Prodromou, C., Liao, C., Hu, B., Mark Roe, S., Vaughan, C. K., Vlasic, I., Panaretou, B., Piper, P. W., and Pearl, L. H. (2004) Structural basis for recruitment of the ATPase activator Aha1 to the Hsp90 chaperone machinery. *EMBO J. 23*, 511−519.
(29) Hutagalung, A. H., and Novick, P. J. (2011) Role of Rab GTPases in membrane traffic and cell physiology. *Physiol. Rev. 91*, 119−149.
(30) Schmoranzer, J., Kreitzer, G., and Simon, S. M. (2003) Migrating fibroblasts perform polarized, microtubule-dependent exocytosis towards the leading edge. *J. Cell Sci. 116*, 4513−4519.
(31) Xu, W., Mollapour, M., Prodromou, C., Wang, S., Scroggins, B. T., Palchick, Z., Beebe, K., Siderius, M., Lee, M. J., Couvillon, A., Trepel, J. B., Miyata, Y., Matts, R., and Neckers, L. (2012) Dynamic tyrosine phosphorylation modulates cycling of the HSP90-P50-(CDC37)-AHA1 chaperone machine. *Mol. Cell 47*, 434−443.
(32) Etienne-Manneville, S. (2013) Microtubules in cell migration. *Annu. Rev. Cell Dev. Biol. 29*, 471−499.
(33) Hopkins, C. R., Gibson, A., Shipman, M., Strickland, D. K., and Trowbridge, I. S. (1994) In migrating fibroblasts, recycling receptors are concentrated in narrow tubules in the pericentriolar area, and then routed to the plasma membrane of the leading lamella. *J. Cell Biol. 125*, 1265−1274.
(34) Bretscher, M. S. (2008) Exocytosis provides the membrane for protrusion, at least in migrating fibroblasts. *Nat. Rev. Mol. Cell Biol. 9*, 916.
(35) Zuo, X., Zhang, J., Zhang, Y., Hsu, S. C., Zhou, D., and Guo, W. (2006) Exo70 interacts with the Arp2/3 complex and regulates cell migration. *Nat. Cell Biol. 8*, 1383−1388.
(36) Thao, N. P., Chen, L., Nakashima, A., Hara, S., Umemura, K., Takahashi, A., Shirasu, K., Kawasaki, T., and Shimamoto, K. (2007) RAR1 and HSP90 form a complex with Rac/Rop GTPase and function in innate-immune responses in rice. *Plant Cell. 19*, 4035−4045.
(37) Eskew, J. D., Sadikot, T., Morales, P., Duren, A., Dunwiddie, I., Swink, M., Zhang, X., Hembruff, S., Donnelly, A., Rajewski, R. A., Blagg, B. S., Manjarrez, J. R., Matts, R. L., Holzbeierlein, J. M., and Vielhauer, G. A. (2011) Development and characterization of a novel C-terminal inhibitor of Hsp90 in androgen dependent and independent prostate cancer cells. *BMC Cancer 11*, No. 468.
(38) Marcu, M. G., Schulte, T. W., and Neckers, L. (2000) Novobiocin and related coumarins and depletion of heat shock protein 90-dependent signaling proteins. *J. Natl. Cancer Inst. 92*, 242−248.
(39) Shelton, S. N., Shawgo, M. E., Matthews, S. B., Lu, Y., Donnelly, A. C., Szabla, K., Tanol, M., Vielhauer, G. A., Rajewski, R. A., Matts, R. L., Blagg, B. S., and Robertson, J. D. (2009) KU135, a novel novobiocin-derived C-terminal inhibitor of the 90-kDa heat shock protein, exerts potent antiproliferative effects in human leukemic cells. *Mol. Pharmacol. 76*, 1314−1322.
(40) Pearl, L. H., and Prodromou, C. (2000) Structure and in vivo function of Hsp90. *Curr. Opin Struct Biol. 10*, 46−51.
(41) Pearl, L. H., Prodromou, C., and Workman, P. (2008) The Hsp90 molecular chaperone: an open and shut case for treatment. *Biochem. J. 410*, 439−453.
(42) Peterson, L. B., and Blagg, B. S. (2009) To fold or not to fold: Modulation and consequences of Hsp90 inhibition. *Future Med. Chem. 1*, 267−283.
(43) Donnelly, A., and Blagg, B. S. (2008) Novobiocin and additional inhibitors of the Hsp90 C-terminal nucleotide-binding pocket. *Curr. Med. Chem. 15*, 2702−2717.
(44) Matts, R. L., Dixit, A., Peterson, L. B., Sun, L., Voruganti, S., Kalyanaraman, P., Hartson, S. D., Verkhivker, G. M., and Blagg, B. S. (2011) Elucidation of the Hsp90 C-terminal inhibitor binding site. *ACS Chem. Biol. 6*, 800−807.
(45) Meyer, P., Prodromou, C., Liao, C., Hu, B., Roe, S. M., Vaughan, C. K., Vlasic, I., Panaretou, B., Piper, P. W., and Pearl, L. H. (2004) Structural basis for recruitment of the ATPase activator Aha1 to the Hsp90 chaperone machinery. *EMBO J. 23*, 1402−1410.
(46) Samadi, A. K., Zhang, X., Mukerji, R., Donnelly, A. C., Blagg, B. S., and Cohen, M. S. (2011) A novel C-terminal HSP90 inhibitor KU135 induces apoptosis and cell cycle arrest in melanoma cells. *Cancer Lett. 312*, 158−167.
(47) Chen, W. S., Chen, C. C., Chen, L. L., Lee, C. C., and Huang, T. S. (2013) Secreted heat shock protein 90alpha (HSP90alpha) induces nuclear factor-kappaB-mediated TCF12 protein expression to down-regulate E-cadherin and to enhance colorectal cancer cell migration and invasion. *J. Biol. Chem. 288*, 9001−9010.

(48) Peterson, L. B., Eskew, J. D., Vielhauer, G. A., and Blagg, B. S. (2012) The hERG channel is dependent upon the Hsp90alpha isoform for maturation and trafficking. *Mol. Pharmaceutics 9*, 1841−1846.
(49) Zhang, L., Zhao, H., Blagg, B. S., and Dobrowsky, R. T. (2012) C-terminal heat shock protein 90 inhibitor decreases hyperglycemia-induced oxidative stress and improves mitochondrial bioenergetics in sensory neurons. *J. Proteome Res. 11*, 2581−2593.